Research Journal of Applied Science, Engineering and Technology 3(4): 337-343, 2011
ISSN: 2040-7467

Received: March 07, 2011 Accepted: April 07, 2011 Published: April 20, 2011

Characterization of the Minimum Effective Layer of Thermal Insulation Material Tow-plaster from the Method of Thermal Impedance

[1]M.S. Ould Brahim, [1]I. Diagne, [2]S. Tamba, [3]F. Niang and [1]G. Sissoko
[1]Laboratory of Semiconductors and Solar Energy, Physics Department, Faculty of Science and Technology, University Cheikh Anta Diop, Dakar, Senegal
[2]Civil Engineering Department, Ecole Polytechnique de Thiès, Sénégal
[3]IUT/UT, University Thies, Thies, Senegal

Abstract: Our objective in this study is to determine the effective thermal insulating layer of a composite tow-plaster. The characterization of thermal insulating material is proposed from the study of the thermal impedance in dynamic two-dimensional frequency. Thermo physical properties of the material tow-plaster are determined from the study of the thermal impedance. Nyquist representations have introduced an interpretation of certain phenomena of heat transfer from the series and shunt resistors. The overall coefficient of heat exchange is determined from the Bode plots. A method for determining the thermal conductivity is proposed.

Key words: Frequency dynamic regime, thermal impedance, Nyquist representation, effective thermal insulation layer

INTRODUCTION

Thermal comfort in buildings (Tamba *et al*., 2007) requires good thermal insulation. Tow (the tow is made up of filaments, hemp, flax, etc.. prepared to be spun), biodegradable natural product is used as thermal insulation in combination with the plaster as a binder. Thermo physical characteristics (thermal conductivity l » 0.15W/m°C; coefficient of thermal diffusivity α » $2.07.10^{-7}m^2/s$) (Voumbo, 2008) of a tow-plaster material are measured.

Several methods for determining the thermal conductivity of materials are proposed. Jannot *et al*. (2009) proposes a technique for determining the thermal conductivity of insulating materials with low density. The three-dimensional modeling system is used for sensitivity analysis. The estimation method is described and applied to experimental measurements performed at atmospheric pressure and vacuum.

Bekkouche *et al*. (2007) studied the effect of thermal insulation on a piece of habitat in a region of Algeria. The simulation study showed the effect of thermal barrier that influences on the insulation a sunny wall.

In this study, a simulation technique is proposed to characterize the heat transfer through the material from the study of the thermal impedance. Nyquist representations (Dieng *et al*., 2007) have characterized some thermal phenomena in the determination of series resistance and shunt. Bode diagrams helped give the limits of the overall coefficient of heat exchange and propose a technique to derive the thermal conductivity of thermal insulating material.

Theory:

Study design: The study device, Fig. 1a, is a material made of tow and plaster of parallelepiped shape whose thermo physical properties (thermal conductivity and thermal diffusivity coefficient) (Gaye *et al*., 2001) are determined.

The tow-plaster material, Fig. 1b, is subject to a side in contact with the outdoor environment: climatic solicitation (temperature, fluid motion outside) under dynamic frequency regime. The other side of the material is isolated environment where the temperature is changing in dynamic frequency regime established. The heat exchange is assumed at lower level of this face.

Through the heat exchange coefficients (h_{1y}, h_{2y}, h_{1x}, h_{2x}) the material acquires or disposes of the heat, which translates into a temperature change in the material.

The climatic solicitation conditions are imposed along the depth (Oy) of the material. Both parties are defined in the material of the thermal response: the area sensitive to climate solicitation and thermal insulation layer effectively.

The evolution of heat along the axis (Ox) reflects lateral losses of heat through the material, the heat transfer coefficients h1x and h2x are supposed to ignore low heat exchanges on the sides.

Thermal impedance of the material:

Temperature and heat flux density in the material: The temperature T(x, y,ω , t) of the tow-plaster material is defined by the heat Eq. (1), without heat source and then. The temperature of the material is essentially exchanges heat to walls of the material.

Corresponding Author: G. Sissoko, Laboratory of Semiconductors and Solar Energy, Physics Department, Faculty of Science and Technology, University Cheikh Anta Diop, Dakar, Senegal

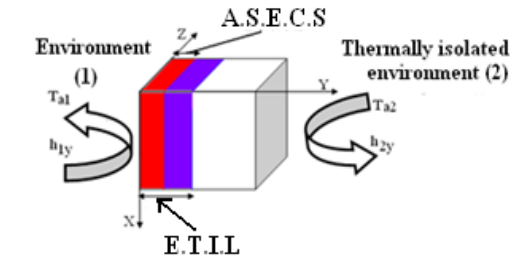

(a)

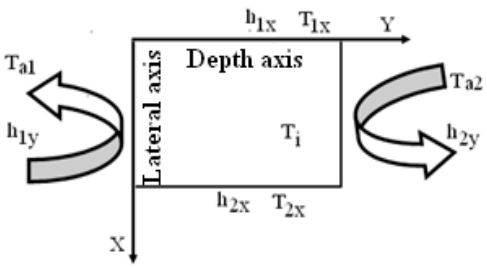

(b)

Fig. 1: Model to study the material tow-plaster; (a) Material having three-dimensional, (b) material

$$\frac{\partial^2 T}{\partial x^2} + \frac{\partial^2 T}{\partial y^2} - \frac{1}{\alpha}\frac{\partial T}{\partial t} = 0 \qquad (1)$$

$$\alpha = \frac{\lambda}{\rho.C} \qquad (2)$$

The tow-plaster material is subject to the following boundary conditions:

$$\lambda.\left.\frac{\partial T(x,y,t)}{\partial x}\right|_{x=0} = h_{1x}\left[T(0,y,t) - 0\right] \qquad (3)$$

$$-\lambda.\left.\frac{\partial T(x,y,t)}{\partial x}\right|_{x=L} = h_{2x}\left[T(L,y,t) - 0\right] \qquad (4)$$

$$\lambda.\left.\frac{\partial T(x,y,t)}{\partial y}\right|_{y=0} = h_{1y}\left[T(x,0,t) - T_{a1}\right] \qquad (5)$$

$$-\lambda.\left.\frac{\partial T(x,y,t)}{\partial y}\right|_{y=h} = h_{2y}\left[T(x,H,t) - T_{a2}\right] \qquad (6)$$

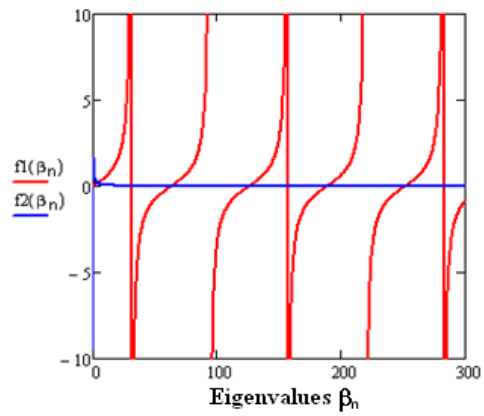

Fig. 2: Graphic determination of the eigenvalues β_n

In dynamic frequency and given boundary conditions imposed on the system, we get the expression in annex (1) temperature T(x,y,ω,t)

μ_n and β_n are constants constituting the eigenvalues related by Eq. (8) and determined graphically from Fig. 2 by considering the transcendental Eq. (9).

$$\mu_n = \sqrt{\beta_n^2 + \frac{i.\omega}{\alpha}} = \sqrt{\beta_n^2 + \frac{\omega}{2.\alpha}(1+i)^2} \qquad (8)$$

$$\tan(\beta_n.L) = \frac{\lambda.\beta_n(h_{1x} + h_{2x})}{(\lambda.\beta_n)^2 - h_{1x}.h_{2x}} \qquad (9)$$

$$f_1(\beta_n) = \tan(\beta_n.L) \qquad (10)$$

$$f_2(\beta_n) = \frac{\lambda.\beta_n(h_{1x} + h_{2x})}{(\lambda.\beta_n)^2 - h_{1x}.h_{2x}} \qquad (11)$$

Table 1 Summarizes some eigenvalues bn from which the temperature of the insulation plaster tow followed.

The boundary conditions (5) and (6) to determine the constants a_n and b_n, respectively in expressions Appendix, Eq. (2) and (3) are involved in the expression of the temperature.

From the relation of Fourier (Meukam *et al*., 2004) defining the flux density of heat conduction in the material, we give the expression (14), the density of heat flow in the tow- plaster insulating.

Thermal impedance of the tow-plaster material: The thermal impedance Z (x, y, w) (annex 6) (Bourouga *et al*., 2000) is defined in Eq. (16) as the ratio of temperature variation DT(x,y,w,t) between a position in front of coordinates (x, 0) and an inner position of the

Table 1: Eigenvalues b_n determined graphically. $h_{1x} = h_{2x} =$ 0.05 W/m².°C ; l » 0.15 W/m².°C.

n	1	2	3	4	5	6	7	8	9	10	11	12
β_n	5	65	127	189	250	314	378	441	505	566	629	692

material coordinates (x, y) on the density of heat flow ψ(x, y, w, t), (annex 5) passing through this portion of the material.

$$Z(x,y,\omega) = \frac{\Delta T}{\psi} \qquad (16)$$

Expression, annex 6, corresponds to the thermal impedance of the material in dynamic frequency regime.

RESULTS

Evolution of temperature and density of heat flow: For an effective thermal insulation layer (E.T.I.L) (Voumbo *et al*., 2010a, b), e = 2 cm, Figure 3 shows the changes in temperature, curve (2), and the density of heat flow curve (1) through the thermal insulating plaster-tow in function of the excitation pulse.

For low values of pulse excitation, $\omega < 10^{-4}$ rad/s, temperature T is high, which corresponds to a density of heat flow in the relatively weak material. For these low values of pulse excitation, the material does not good thermal insulator.

Beyond a pulse excitation $\omega > 10^{-4}$ rad/s, the material temperature decreases significantly while the density of heat flow ψ increases and reaches a maximum corresponding to an optimal value of the excitation pulse $\omega_{iop} = 6.46.10^{-4}$ rad/ for an experimental period τ = 02 h 40 min of exterior climatic solicitation providing optimal thermal insulation. Note that the optimal excitation pulse ω_{iop} corresponds to the temperature curve at an inflection point corresponding to minimum temperature insulation inside the middle T ≤ 9,5°C = 282.65 K.

For higher excitation pulses above ω_{iop}, the temperature and heat flux density decrease and evolve in the same manner as characterizing a very good performance thermal insulation for the effective thermal insulating layer considered and periods of climatic solicitations exterior τ < 02h40 min.

The characteristic of temperature variation - density of heat flux: The Fig. 4 defined the thermal impedance of thermal insulating material from the evolution of the temperature variation (ΔT = T(x, y = 0) - T(x, y) depending on the density of heat flow ψ through the material. The curves of this figure have the same profile and define at any point an operating point characterized by dynamic thermal impedance Z.

Consider a thin layer δy ≈ ε (ε→0), near the face subject to climatic solicitations exterior ΔT= T(x, y=0) -

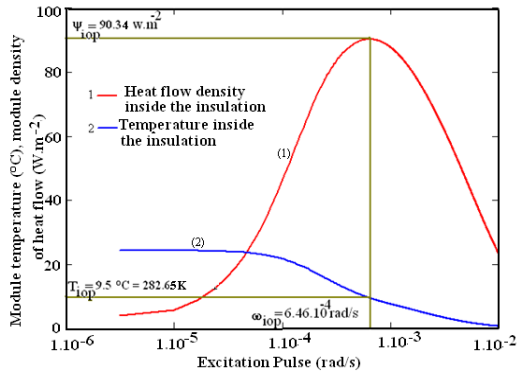

Fig. 3: Evolution of the density of heat flow and temperature inside the insulating function of the excitation pulse; x = 0.025 m, y = 0.02 m; h_{1y} = 50 W/m².°C ; h_{2y} = 0.05 W/m².°C ; T_{o1} = 25°C ; T_{o2} = 10°C

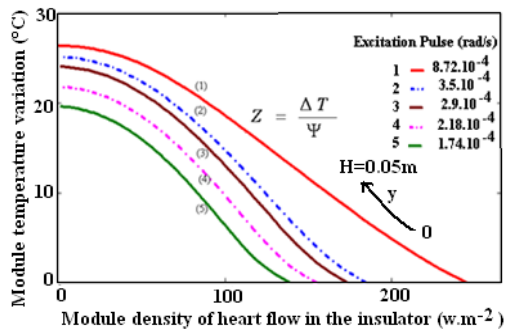

Fig. 4: Characteristic temperature variation - heat flux density; influences the pulse excitation. x = 0.05 m; h_{1y} = 50 W/m².°C; h_{2y} = 0.05 W/m².°C; T_{o1}= 25°C; T_{o2}= 10°C

T(x, y = ε) ≈ 0. This corresponds to almost zero thermal impedance Z resulting in an important passage of heat flux density (short circuit current of electricity).

In depth for a position y » H - e, we have ΔT =T(x, y = 0) - T(x, y =H-ε) ≈ T(x, y = 0); the thermal impedance Z of the material is the maximum heat flux density vanishes (ΔT corresponds to an open circuit voltage).

The thermal impedance Z of thermal insulating material can thus characterized the thermal behavior of materials from its study.

Bode diagram of the thermal impedance: The evolution of the modulus of the thermal impedance as a function of the excitation pulse for different values of thickness Δy = y - 0 = y, is given in Fig. 5.

The curves show two profiles characterizing two main areas of thermal insulating material according to the exterior climatic solicitations:

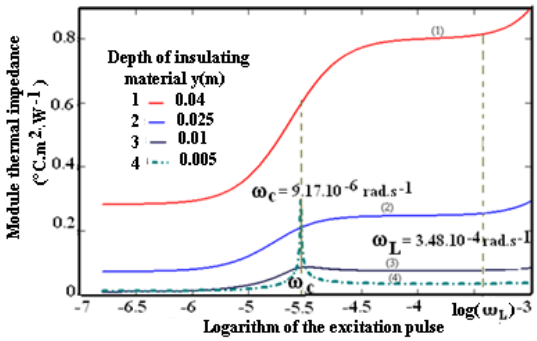

Fig. 5: The behavior of the impedance versus the logarithm of the excitation pulse, influence of the depth of the insulating material. x = 0.025 m; h_{1y} = 50 W/m^2. °C; h_{2y} = 0.05 W/m^2.°C; T_{o1} = 25°C ; T_{o2} = 10°C

- Area Sensitive to Exterior Climate Solicitations, A.S.E.C.S, $\Delta y \approx 5$ mm, curve (4): the variation of thermal impedance module is relatively low: the layer absorbs a significant amount of heat causing the wall heat and presents a important jump for the cut-off pulse $\omega_c \approx 10^{-5}$ rad/s.
- The effective thermal insulation layer, E.T.I.L, for $\Delta y \geq 1$ cm; curves (1), (2) and (3) have the same profile; thermal impedance is constant and small for low values of the pulsation and high and constant values of the relatively large excitation pulse. The curves show a cut-off pulse $\omega_c \approx 10^{-5}$ rad/s, comparable to that obtained in the A.S.E.C.S.

For $\omega \geq \omega_L \approx 3.48.10^{-4}$ rad/s, the thermal impedance modulus increases with the exciter pulse, the heat flux density decreasing significantly in the material; the temperature positions increase in the E.T.I.L virtually zero.

Table 2 summarizes some values limit of the thermal impedance in A.S.E.C.S and E.T.I.L.

Determination of series resistance and shunt: Nyquist representations of the thermal impedance give the evolution of the imaginary part of impedance as a function of the real part.

Figure 6a identifies the values of series resistors R_s ($\omega \to 0$), shunt R_{sh} (from the cutoff frequency of giving $R_{sh}/2$), thermal resistance $R_s+R_{sh} = R_{th,}$ and limit thermal resistance R_L ($\omega \to \omega_L$).

$R_L \leq R_{th,}$; R_L is the thermal resistance characterizing the phenomena of heat transfer to the wall material (heat exchange coefficients, pulse excitation) and heat transfer by conduction in the material (thermal conductivity of the insulation).

The curves (1), (2) and (3) of Fig. 6a, show that the resistance values (R_s, R_{sh}, R_{th} et R_L) increase with the thickness Dy = y – 0 = y, increased thermal resistance

Table 2: Limit values of the impedance modulus with depth

		$\omega \to 0$	$\omega \to \omega_c$	$\omega \to \omega_L$
|Ze|(°C.m^2.W^{-1})	y = 0.5 cm	0.013	0.301	0.035
	y = 1.0 cm	0.013	0.085	0.075
	y = 2.5 cm	0.072	0.210	0.253
	y = 4.0 cm	0.282	0.595	0.812

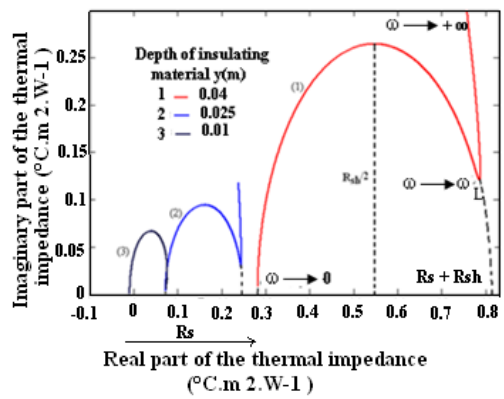

Fig. 6a: Evolution of the imaginary part of the thermal impedance according to its real part, influence of depth, X = 0.025 m; h_{1y} = 50 W/m^2 °C; h_{2y} = 0.05 W/m^2.°C; T_{o1} = 25°C; T_{o2} = 10°C

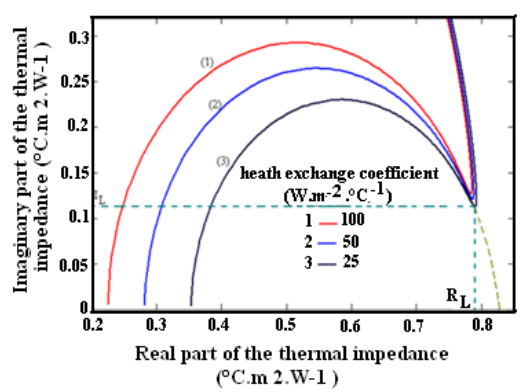

Fig. 6b: Evolution of the imaginary part of the thermal impedance according to its real part, influence of heat exchange coefficient, x = 0.025 m; y = 0.04 m; h_{2y} = 0.05 W/m^2.°C; T_{o1} = 25°C; T_{o2} = 10°C

resulting in substantial loss of heat flux density in the material corresponding to a favorable feature of the insulation.

The curve (3) has a negative value of R_s, reflecting, for A.S.E.C.S, relaxation phenomena; some of the heat received by the insulator is pushed to the outside environment through heat exchange coefficient.

Figure 6b shows the influence of heat transfer coefficients on the values of series resistance and shunt. The series resistance decreases as the heat transfer rate increases as opposed to the shunt resistor.

Table 3 shows some values of resistors (R_s, R_{sh}, R_{th} et R_L) and shows their evolution as a function of the

Table 3: Values of shunt and series resistances with depth and the coefficient of heat exchange

		h_{1y} = 25 W/m^2.ºC	h_{1y} = 50 W/m^2.ºC	h_{1y} =100 W/m^2.ºC
y = 1.0 cm	R_s	0.0074	- 0.008	- 0.019
	R_{sh}	0.066	0.082	0.093
	$R_s + R_{sh}$	0.074	0.074	0.074
	R_L ($\omega \rightarrow \omega_L$)	0.074	0.074	0.074
y = 2.5 cm	R_s	0.111	0.072	0.044
	R_{sh}	0.144	0.188	0.222
	$R_s + R_{sh}$	0.255	0.260	0.266
	R_L ($\omega \rightarrow \omega_L$)	0.246	0.245	0.243
y = 4.0 cm	R_s	0.354	0.282	0.225
	R_{sh}	0.460	0.530	0.585
	$R_s + R_{sh}$	0.814	0.812	0.810
	R_L ($\omega \rightarrow \omega_L$)	0.790	0.788	0.785

Table 4: Comparison of the limits values of the overall coefficient of heat exchange with respect to

	$\omega \rightarrow 0$		$\omega \rightarrow \omega_c$		$\omega \rightarrow \omega_L$	
	K(W / m^2.ºC)	λ/y(W / m^2.ºC)	K(W / m^2.ºC)	λ/y (W / m^2.ºC)	K(W / m^2.ºC)	λ/y (W / m^2.ºC)
y = 0.5 cm	76.9	30	3.3	30	28.6	30
y = 1.0 cm	76.9	15	11.7	15	13.3	15
y = 2.5 cm	13.9	6	4.7	6	3.9	6
y = 4.0 cm	3.5	3.75	1.7	3.75	1.2	3.75

thickness of the insulation Dy = y - 0 = y, and heat exchange coefficients.

DISCUSSION

The heat transfer through the material is characterized by the overall coefficient of heat transfer defined by the expression K = 1 / |Z|. The overall coefficient of heat exchange K depends on heat transfer, thermal conductivity l and pulse excitation w.

Table 4 below gives the limits for the overall heat transfer coefficient obtained from Table 2.

- For $\omega \rightarrow 0$, the overall coefficient of heat exchange is very large relative to λ/y; the contribution of heat transfer coefficients by convection is relatively large; flux density of heat absorbed by the material is important.
- For $\omega \rightarrow \omega_c$, the overall coefficient of heat exchange is minimal and less than λ/y; the material gives up heat by relaxation phenomena accentuated for small thicknesses of material ($R_s < 0$ for $y \leq 0.5$ cm).
- For $\omega \rightarrow \omega_L$, considering the relatively low values of insulation thickness, $\Delta y = y - 0 = y \leq 0.5$ cm, the overall coefficient of heat transfer is comparable to λ/y with a maximum relative uncertainty 4.67%. This allows a determination of thermal conductivity λ of the thermal insulating material.

The uncertainty becomes increasingly important when the thickness of the material increases.

CONCLUSION

The study of heat transfer from the thermal impedance in the dynamic frequency regime has allowed to highlighting two important parts of the thermal insulating material:

- Area Sensitive to Exterior Climate Solicitations (A.S.E.C.S)
- Effective thermal insulating layer (E.T.I.L)

The Bode plots were used to determine respectively the limit values of the thermal impedance and hence the overall coefficient of heat transfer under certain conditions allowing access to the thermal conductivity of the material.

Nyquist representations have determined the values of series resistance, shunt resistance and the limit value thermal resistance.

NOMENCLATURE

Latin letters:

C specific heat, m^2/s^2.ºC
L width of the material, m
H material thickness, m
H heat exchange coefficient, W/m^2.ºC
K overall coefficient of heat exchange, W/m^2.ºC
R_{th} thermal resistance, ºC.m^2/W
R_L thermal boundary resistance, ºC.m^2/W
R_S series resistor, ºC.m^2/W
R_{sh} shunt resistor, ºC.m^2/W
T temperature, ºC, K
T(K) = T(ºC) + 273.15
1cm = 10^{-2} m
x,y Cartesian coordinate, m
Z Thermal impedance, ºC.m^2/W
E.T.I.L: Effective Thermal Insulation Layer

A.S.E.C.S: Area Sensitive to Exterior Climate Solicitations

Greek letters:
ψ heat flux density, W/m^2
λ thermal conductivity, W/m.K
ρ density, kg/m^3
α coefficient of thermal diffusivity, m^2/s
ω pulse excitation, rad/s
τ solicitation period climate, hour
Indexes/Exhibitors:
i = 1,2 extern

Appendix:

$$T(x,y,\omega,t) = \left[\sum_n (\cos(\beta_n.x) + \frac{h_{1x}}{\lambda.\beta_n}.\sin(\beta_n.x)) \times (a_n.\cosh(\mu_n.y) + b_n.\sinh(\mu_n.y))\right].e^{i.\omega.t} \quad (1)$$

$$a_n = \frac{4.\lambda.\beta_n.\sin(\beta_n L)\left[h_{1y}.(\lambda.\mu_n.ch(\mu_n.H) + h_{2y}.sh(\mu_n.H)).T_{01} + h_{2y}.\lambda.\mu_n.T\right]}{D_n\left[h_{1y}(\lambda.\mu_n.ch(\mu_n.H) + h_{2y}.sh(\mu_n.H)) + \lambda.\mu_n(\lambda.\mu_n.sh(\mu_n.H) + h_{2y}.ch(\mu_n.H))\right]} \quad (2)$$

$$b_n = \frac{h_{1y}.4.\lambda.\beta_n.\sin(\beta_n L).\left[h_{2y}.T_{02} - (\lambda.\mu_n.sh(\mu_n.H) + h_{2y}.ch(\mu_n.H)).T_{01}\right]}{D_n\left[h_{1y}(\lambda.\mu_n.ch(\mu_n.H) + h_{2y}.sh(\mu_n.H)) + \lambda.\mu_n(\lambda.\mu_n.sh(\mu_n.H) + h_{2y}.ch(\mu_n.H))\right]} \quad (3)$$

$$D_n = \lambda.\beta_n.(\sin(2\beta_n L) + 2\beta_n L) + h_{1x}.(1 - \cos(2\beta_n L)) \quad (4)$$

$$\psi(x,y,\omega,t) = \lambda.\left[\begin{array}{l} \mu_n^2.\left(\sum_n \cos(\beta_n.x) + \frac{h_{1x}}{\lambda.\beta_n}.\sin(\beta_n.x)).(a_n.sh(\mu_n.y) + b_n.ch(\mu_n.y))\right)^2 \\ + \beta_n^2.\left(\sum_n (-\sin(\beta_n.x) + \frac{h_{1x}}{\lambda.\beta_n}.\cos(\beta_n.x)).(a_n.ch(\mu_n.y) + b_n.sh(\mu_n.y))\right)^2 \end{array}\right]^{\frac{1}{2}}.e^{i.\omega.t} \quad (5)$$

$$Z(x,y,\omega) = \frac{\sum_n \left[a_n(\cos(\beta_n.x) + \frac{h_{1x}}{\lambda.\beta_n}.\sin(\beta_n.x)) - (\cos(\beta_n.x) + \frac{h_{1x}}{\lambda.\beta_n}.\sin(\beta_n.x)).(a_n.\cosh(\mu_n.y) + b_n.\sinh(\mu_n.y))\right]}{\lambda.\left[\begin{array}{l} \mu_n^2.\left(\sum_n (\cos(\beta_n.x) + \frac{h_{1x}}{\lambda.\beta_n}.\sin(\beta_n.x)).(a_n.sh(\mu_n.y) + b_n.ch(\mu_n.y))\right)^2 \\ + \beta_n^2.\left(\sum_n - \sin(\beta_n.x) + \frac{h_{1x}}{\lambda.\beta_n}.\cos(\beta_n.x)).(a_n.ch(\mu_n.y) + b_n.sh(\mu_n.y))\right)^2 \end{array}\right]^{\frac{1}{2}}} \quad (6)$$

ACKNOWLEDGMENT

We thank all the authors cited in references; their work we are a very big contribution. We also thank the members of the international group of research renewable energy of laboratory of semiconductors and solar energy at the University Cheikh Anta Diop in Dakar.

REFERENCES

Bekkouche, S.M.A., T. Benouaz and A. Cheknane, 2007. Simulation study of the effect of thermal insulation of a piece of habitat in the region of Ghardaia. Revue des Energies Renouvelables, 10(2): 281-292.

Bourouga, B., V. Goizet and J.P. Bardon, 2000. The theory governing the instrumentation of a thermal sensor parietal low inertia. Int. J. Therm. Sci., 39: 96-109.

Dieng, A., L. Ould Habiboulahy, A.S. Maïga, A. Diao and G. Sissoko, 2007. Impedance spectroscopy method applied to electrical parameters determination on bifacial silicon solar cell under magnetic field. J. Sci., 7(3): 48-52.

Gaye, S., F. Niang, I. K. Cissé, M. Adj, G. Menguy and G. Sissoko, 2001. Characterisation of thermal and mechanical properties of polymer concrete recycled. J. Sci., 1(1): 53-66.

Jannot, Y., A. Degiovanni and G. Payet, 2009. Thermal conductivity measurement of insulating materials with a three layers device. Int. J. Heat Mass Tran., 52: 1105-1111.

Meukam, P., Y. Jannot, A. Noumow and T.C. Kofan, 2004. Thermo physical characteristics of economical building materials. Constr. Build. Mater., 18: 437-443.

Tamba, S., L.M. Voumbo, A. Wereme, S. Gaye and G. Sissoko, 2007. Durability of lightweight concrete made from wood chips. J. Sci., 7(4): 67-72.

Voumbo, M.L., 2008. Contribution to the study of thermophysical characteristics of local materials: Application to kapok. Ph.D., FST/UCAD, Senegal.

Voumbo, M.L., A. Wareme, S. Gaye, M. Adji and G. Sissoko, 2010a. Characterization of the thermophysical properties of kapok. Res. J. Appl. Sci. Eng. Technol., 2(2): 143-148.

Voumbo, M. L., A. Wareme and G. Sissoko, 2010b. Characterization of Local Insulators: Sawdust and Wool of Kapok. Res. J. Appl. Sci. Eng. Technol., 2(2): 138-142.